DOI: 10.1002/ejic.201100829

A New Route to Lead Chalcogenide Nanocrystals

Karthik Ramasamy,[a] Ayorinde Olufunke Nejo,[b] Nonto Ziqubu,[b] Pullabhotla V. S. R. Rajasekhar,[b] Adeola A. Nejo,[b] Neerish Revaprasadu,*[b] and Paul O'Brien[a]

Keywords: Lead / Chalcogens / Nanostructures / Electron microscopy

Nanoparticles of lead sulfide, selenide and telluride have been synthesized by the reduction of sulfur, selenium or tellurium powder with sodium borohydride ($NaBH_4$) to produce sulfide, selenide or telluride ions, followed by their reaction with a lead salt. In comparison to the chloride, nitrate or sulfate, considerable control of the product is possible when lead carbonate is used as the salt; various shapes of nanoparticles are obtained on varying temperatures and/or times of reaction. The nanoparticles were characterized by infrared spectroscopy (IR), powder X-ray diffraction (PXRD), transmission electron microscopy (TEM), high resolution transmission electron microscopy (HRTEM) and X-ray photoelectron spectroscopy (XPS).

Introduction

Lead chalcogenide materials with critical dimensions of the order of nanometers have been of considerable interest of late both because of their unique physical and chemical properties and because of a perceived potential for use in a diverse range of applications.[1–3] Such materials can be used in photovoltaic cells,[4] infrared detectors,[5] and thermoelectric devices.[6] Lead chalcogenide nanocrystals exhibit a strong quantum size effect because of the large Bohr radii of both electron and holes [PbS (≈18 nm), PbSe and PbTe (≈46 nm)], which leads to a large confinement energy. Their critical dimensions, especially for selenide and telluride, are greater than in most II–VI and III–V semiconductors (ZnSe, CdSe, CdS, InAs).[7] The stable and tunable emission of NIR-emitting lead chalcogenide quantum dots (QDs) make them suitable for applications in telecommunications (1300–1600 nm), bioimaging (near-IR tissue window 800 and 1100 nm) and solar cells (800–2000 nm).[8]

Various morphologies of PbE (E = S/Se/Te) nanocrystals have been reported, including spheres,[9] cubes,[10] rings,[11] tubes,[12] wires,[13,14] dendrites,[15] and sponge-like structures.[16] Several groups have reported the shape evolution of PbSe nanocrystals from cubes to truncated octahedral,[17] spheres to cubes[18] and stars to cubes.[10] Shape evolution for PbE can be affected by temperature, growth time, solvent and precursor delivery. The systematic tuning of the size and shape of nanocrystallites remains a key objective in realizing both functionality and assembly. The synthesis of such nanocrystals has involved methods that include sputtering,[19] ultrasonic synthesis,[20] injection of a solution of a lead salt and trioctylphosphane chalcogenide (TOP-E, E = S, Se, Te) into a hot solvent,[11,21] thermolysis of single source precursors,[18,22–27] or hydrothermal synthesis.[27,28] These methods generally involve high temperatures and/or quite difficult conditions such as high vacuum or high pressure or salt–solvent-mediated high temperature.

Rhodes et al. demonstrated the triggered aggregation of PbS nanocrystals in a polymer matrix by changing the 1,2-ethanedithiol concentration-triggered assembly of network-like QD structures (low concentration) and self-assembled more-ordered micrometer-sized crystals (high concentration).[29] The role of 1,2-ethanedithiol in decreasing the aggregation as a result of decreasing inter-QD separation and the self-assembly as result of a rapid ligand-exchange process was suggested.[29] The 1D structures from such processes are often polycrystalline and not well dispersed after separating from the template. Limited success has been reported in the growth of 1D PbTe by solution-based soft-templating approaches. In a preliminary work, we demonstrated a simple approach to controlled growth of low-dimension PbTe structures (spheres or rods).[30]

Herein we report further on this methodology and its extension to PbS and PbSe. The method involves the reaction of sulfur, selenium or tellurium powder with sodium

[a] The School of Chemistry and the School of Materials, The University of Manchester, Oxford Road, Manchester, M13 9PL, UK
Fax: +44-161-275-4598
[b] Department of Chemistry, University of Zululand, Private Bag X1001, Kwadlangezwa, 3886, South Africa
Fax: +27-35-902-6568
E-mail: nrevapra@pan.uzulu.ac.za

borohydride ($NaBH_4$) to produce sulfide, selenide or telluride ions, followed by reaction with a lead salt. Considerable control of the reaction is possible when lead carbonate is used as the salt, and various shapes of nanoparticles are obtained at different temperatures and time. We have recently communicated the synthesis of 1D PbTe nanocrystals by this method.[30]

Results and Discussion

Nanoparticles of PbE were synthesized by the addition of an aqueous suspension or solution of a lead salt (chloride, nitrate, sulfate or carbonate) to a freshly prepared NaH(S/Se/Te) solution. The isolated solid product was dispersed into TOP and injected into hot HDA at temperatures of 190, 230 or 270 °C and held at the same temperature for 2–4 h. After cooling to 50 °C, the nanoparticles were isolated by the addition of methanol to the reaction mixture. The sequence of reactions is shown in below equations.

$$4NaBH_4 + 2E + 7H_2O \longrightarrow 2NaHE + Na_2B_4O_7 + 14H_2$$

$$NaHE + PbCO_3 \longrightarrow PbE + NaHCO_3$$

E = S, Se or Te

PbS Nanoparticles

PbS nanoparticles were prepared by the reduction of sulfur by using the above method. The thermolysis reactions were carried out at a reaction temperature of 230 °C. The lead salts, $PbCO_3$, $PbNO_3$ and $PbSO_4$, were used as the lead sources. Figure 1 shows the TEM image of PbS nanoparticles synthesized at 230 °C with $PbCO_3$ as the lead source. The close to cubic particles have an average length of 17 ± 4.7 nm and breadth of 9 ± 2 nm (Figure 1a). The HRTEM image of a single particle shows lattice fringes with a spacing of 3.2 Å, which corresponds to the (111) plane of cubic PbS (Figure 2a). The $PbNO_3$ source also gave elongated particles (Figure 1b). The $PbSO_4$ lead salt gave monodispersed, self–assembled, cubic-shaped particles. The average edge by edge of each cube is 11 nm (Figure 1c). Regular cubes are observed in the HRTEM image (Figure 2b and c). There is a uniform distance of 2.4 nm between the particles. Previous reports suggest that primary amines preferentially coordinate to the [111] facets of PbSe and PbS, which prevents the formation of cubes.[31] In this work, we did not find that the primary amine prevents cube formation. The powder X-ray diffraction pattern (Figure 3a) f the PbS nanoparticles synthesized from the lead carbonate source shows the presence of the (111), (200) and (220) diffraction planes of the cubic rock-salt structure of PbS.

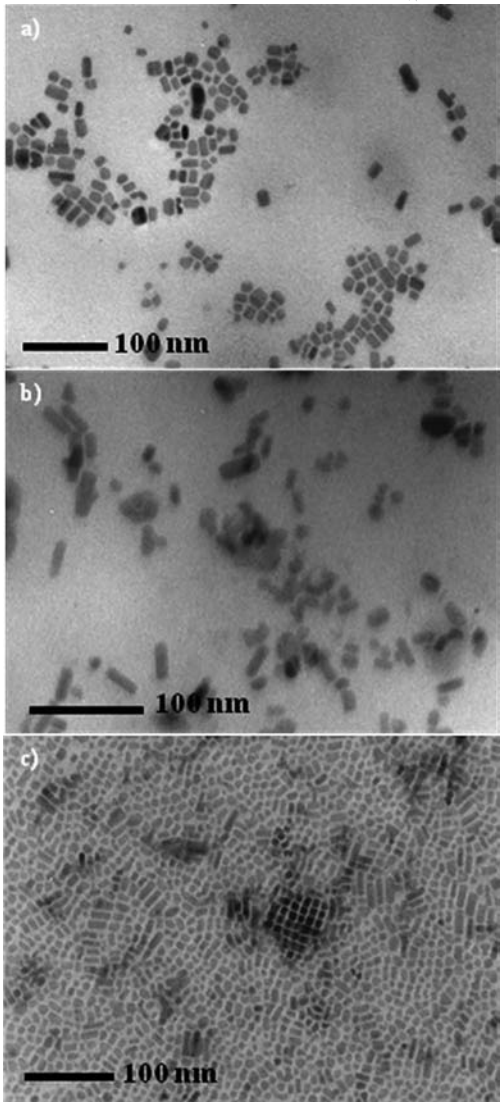

Figure 1. TEM images of PbS nanoparticles prepared at 230 °C from (a) $PbCO_3$, (b) $PbNO_3$ and (c) $PbSO_4$.

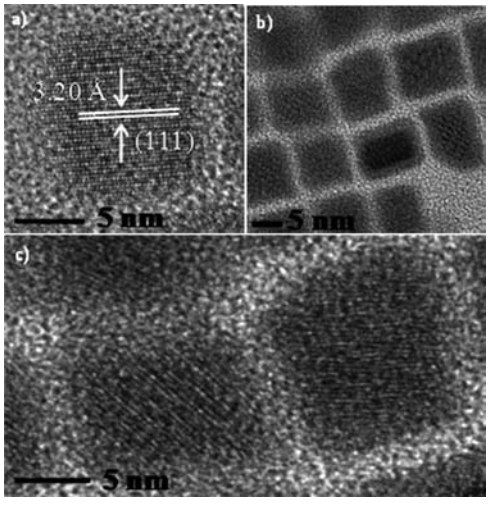

Figure 2. HRTEM images of PbS nanoparticles prepared at 230 °C from (a) $PbCO_3$, (b) and (c) $PbSO_4$.

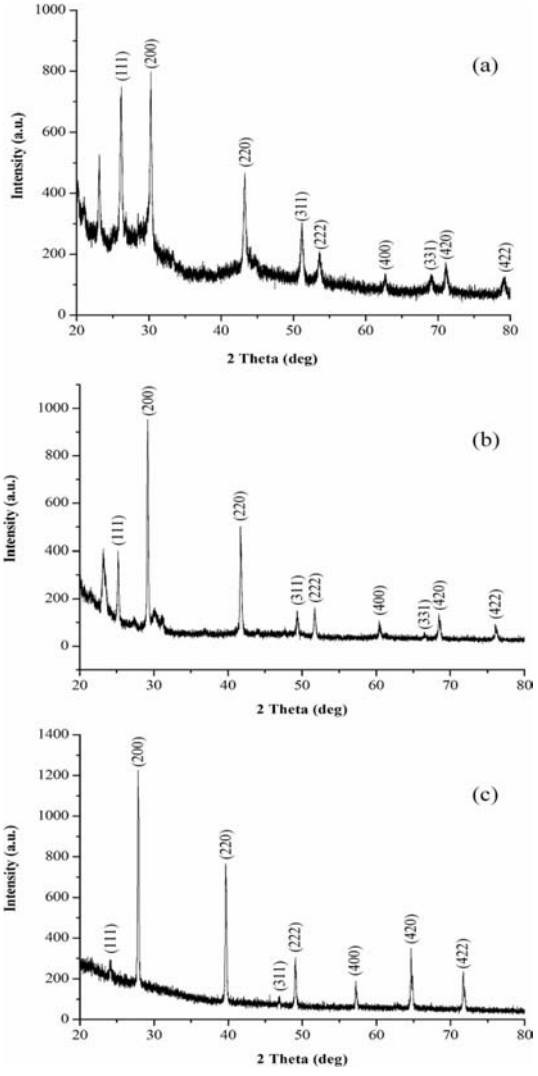

Figure 3. Powder X-ray diffraction patterns of (a) PbS, (b) PbSe and (c) PbTe prepared from $PbCO_3$ at 230 °C.

PbSe Nanoparticles

Figure 4 shows the TEM images of the PbSe particles prepared with $PbCO_3$ at different temperatures. A remarkable change in shape of nanoparticles with temperature was observed. At 190 °C (Figure 4a), monodispersed rods of PbSe nanoparticles were observed with an average width of 12 ± 2 nm and average length of 30 ± 2 nm. At 230 °C, close to perfect cubes were observed with an average size (a) of 15 ± 2 nm (Figure 4c). At the highest temperature of 270 °C, truncated octahedral structures, which tend towards being oblate, are seen with an average size of 20 ± 2 nm (Figure 4e). Factors that control the shapes of inorganic nanocrystals involve competition between thermodynamic and kinetic factors.[32] According to this model, after the formation of a preferred crystalline-phase seed, the final morphology of the nanocrystals is mainly determined by the growth process through a balance between the kinetic growth and thermodynamic preference. At high temperature, the reaction is under thermodynamic control, and the most stable form of the nanocrystal is generally preferred. At lower temperature, the reaction may be under kinetic control, and selective anisotropic growth may occur. In our system for the nanoparticles at 190 °C, kinetically controlled growth on the (100) face is favoured and leads to formation of rods (Figure 4a). When the temperature is increased to 230 °C, the product is controlled by thermodynamics, and the nanoparticles are predominantly cubes (Figure 4c). However, at the highest reaction temperature of 270 °C, a burst of nucleation, which may result in the system growing quickly in both the (111) and (100) planes, leads to truncated octahedral shapes (Figure 4e). Murphy et al.[33] reported that the presence of directing agents, which function as hard or soft templates for the preferential absorption of molecules and ions, directs the growth of nanoparticles into various shapes with gold or silver nanoparticles. We have recently predicted and studied the growth of various shapes of metal–chalcogenide nanoparticles without any template using simple numerical calculations.[34]

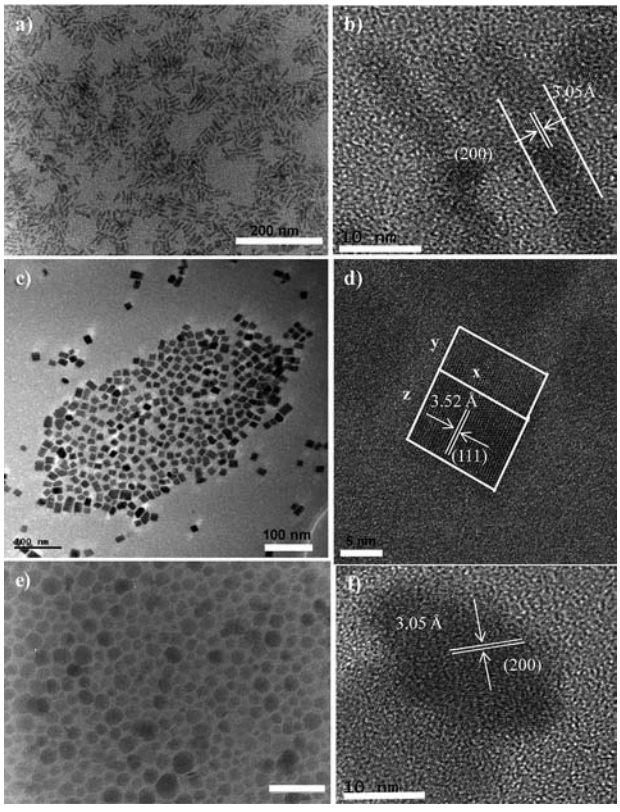

Figure 4. TEM images of PbSe prepared from $PbCO_3$ at (a) 190 °C (rods), (c) 230 °C (cubes) and (e) 270 °C (cuboctahedrons). HRTEM images of PbSe prepared at (b) 190 °C , (d) 230 °C and (f) 270 °C.

The PbSe prepared with $PbCO_3$ nanoparticles were further studied by using HRTEM. The HRTEM images (Figure 4b) of rods obtained at 190 °C show lattice fringes with a d spacing of 3.05 Å, which corresponds to the (100) reflection of cubic PbSe. The HRTEM image of the cubes at 230 °C (Figure 4d) shows lattice fringes with a d spacing of 3.52 Å, which corresponds to the (111) reflection. Lattice fringes of particles prepared at 270 °C have a distance of

3.05 Å, which corresponds to the (100) reflection (Figure 4f).

To fully understand the effect of the lead source on the shape of the synthesized nanoparticles, the reaction was carried out with $PbCl_2$ and $Pb(NO_3)_2$ instead of $PbCO_3$. Figure 5 shows the TEM images of the PbSe nanoparticles obtained with $Pb(NO_3)_2$ as a lead source. At 190 °C, mostly close to perfect cubes with an average size of 15 ± 2 nm (Figure 5a) were obtained; when the reaction temperature was increased to 230 °C, cubes with an average size of 19 ± 1.5 nm (Figure 5b) were obtained. The reaction at 270 °C also gave cubes with a slight increase in the size (21 ± 1 nm) (Figure 5c). Similar cubes of PbSe nanoparticles were obtained in the reaction with $PbCl_2$. The most logical explanation for these observations is that with the soluble salts (chloride and nitrate), the reactions with selenide are essentially complete before injection. The result is fully formed particles, which only yield fairly well-defined cubes. In the case of lead carbonate (probably a suspension of it is formed), only shells are formed on the precursor PbSe surface. On injection, decomposition of the carbonate, with subsequent kinetically controlled growth with different shapes, occurs. The $PbCO_3$ shell on PbSe is confirmed by the FTIR measurement on the intermediate, which shows a common broad peak at 1374 cm^{-1} for lead carbonate and the intermediate, and the disappearance of this broad peak in the spectrum of the final product (Supporting Information). The PbSe nanoparticles were synthesized by using lead chloride, -nitrate and -carbonate as the metal salts. The as-prepared samples of the PbSe nanoparticles with $PbCO_3$ were examined by X-ray powder diffraction to analyze the crystal structures and phase compositions. The XRD patterns (Figure 3b) can be assigned to the face-centred cubic phase of PbSe with a lattice constant of a = 6.124 Å. The major diffraction peaks can be indexed as the (111), (200), (220) and (311) planes of cubic PbSe, which is consistent with values in the standard card (ICDD-78-1903).

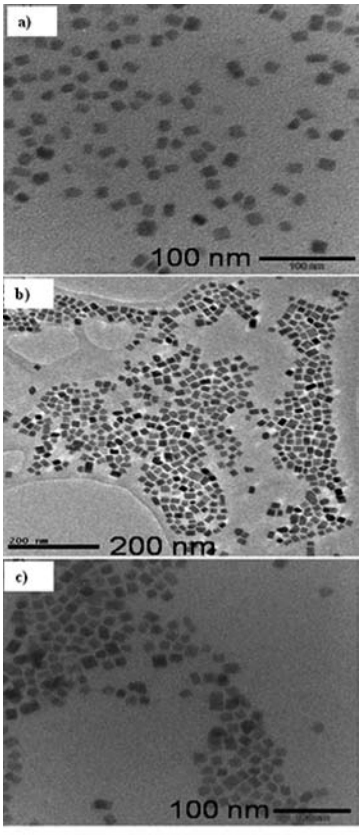

Figure 5. TEM images of PbSe nanoparticles prepared from $Pb(NO_3)_2$ (a) 190 °C, (b) 230 °C and (c) 270 °C.

PbTe Nanoparticles

The PbTe nanoparticles were prepared by the same method, but with tellurium instead of selenium. The PbTe nanocrystals obtained with lead carbonate at different temperatures and reaction times are illustrated in Figure 6. At 190 °C, spherical particles with a diameter of 10.8 ± 1 nm were obtained after 2 h; 4 h gave rods of PbTe with a length of 15 ± 2 nm, width of 5 ± 1 nm (Figure 6a and b). At 230 °C, close to spherical particles with a diameter of 15.2 ± 1 nm were seen at 2 h; rods with a length and width of 35 ± 3 and 8 ± 1 nm respectively, were seen after 4 h (Figure 6c and d). Only rods were obtained at 270 °C with a length of 45 ± 5 nm and width of 7.3 ± 1 nm after 2 h and a length of 51.7 ± 10 nm and a width of 9.1 ± 1.5 nm after 4 h (Figure 6e and f). The PbTe nanoparticles were also prepared with $Pb(NO_3)_2$ and $PbCl_2$. The shape and size of the PbTe nanoparticles obtained by varying the lead salts is

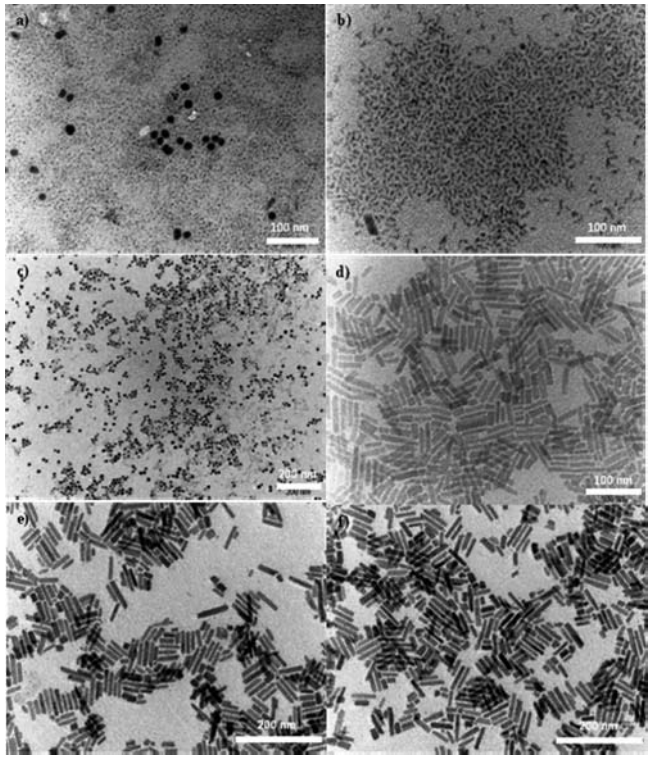

Figure 6. TEM images of PbTe nanocrystals prepared at (a) and (b) 190 °C, (c) and (d) 230 °C, (e) and (f) 270 °C after 2 and 4 h, respectively.

given in Table 1. When $Pb(NO_3)_2$ and $PbCl_2$ were used, mostly spherical particles with an increased size at different temperatures and times were obtained. There was no evidence of anisotropic particle growth with the lead nitrate and -chloride sources (Figure 7). However, lead carbonate gave a distinctly different morphology.

Table 1. Shapes and sizes of PbTe nanocrystals prepared with various lead salts at various temperatures and times.

Lead salt	T	PbTe particles	
	[°C]	After 2 h (av. size, nm)	After 4 h (av. size, nm)
Carbonate	190	spheres (10.8 ± 1)[a]	rods (15 ± 2,[b] 5 ± 1[c])
	230	spheres (15.2 ± 1)[a]	rods (35 ± 3,[b] 8 ± 1[c])
	270	rods (45 ± 5,[b] 7.3 ± 1[c])	rods (51.7 ± 10,[b] 9.1 ± 1[c])
Nitrate	190	spheres (7 ± 1)[a]	spheres (9.2 ± 2)[a]
	230	spheres (8 ± 0.5)[a]	spheres (12.8 ± 1.5)[a]
	270	spheres (11.2 ± 1)[a]	spheres (13.4 ± 2) [a]
Chloride	190	spheres (8 ± 1)[a]	spheres (8.8 ± 1.5)[a]
	230	spheres (10.7 ± 5)[a]	spheres (12.8 ± 2)[a]
	270	spheres (13.8 ± 1)[a]	spheres (15.2 ± 1.5)[a]

[a] Diameter. [b] Length. [c] Width.

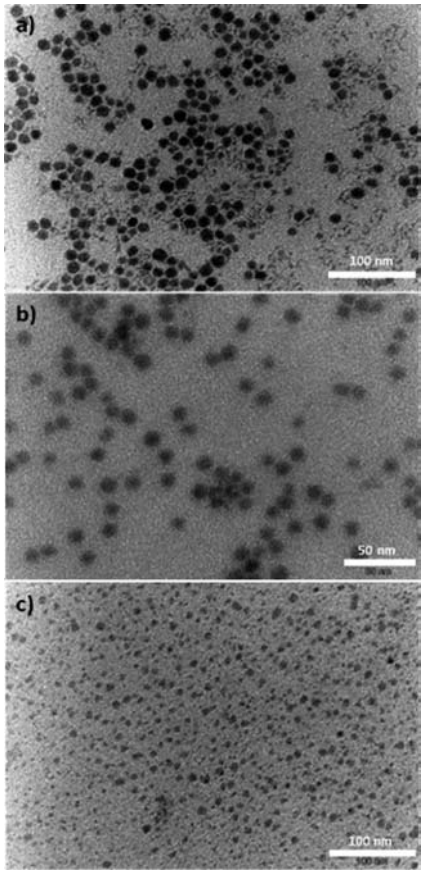

Figure 7. TEM images of PbTe dots prepared at 230 °C after 2 h with (a) $PbCO_3$, (b) $Pb(NO_3)_2$ and (c) $PbCl_2$ as the lead source.

The difference in morphology of the PbTe nanoparticles obtained from the carbonate source relative to those obtained from the chloride and nitrate sources can be attributed to the lower solubility of lead carbonate. This results in a suspension of the lead carbonate, which thereby forms a shell on the PbTe surface. The surface energy of the crystallographic faces of the initially formed seeds has a dominant effect on the anisotropic growth pattern of the nanoparticles. The surfactant, in this case hexadecylamine, can selectively be adsorbed onto the surface, and, thus, the surface energy is modulated. The undissolved lead carbonate also selectively adheres to the surface of the PbTe nanoparticles, and this accentuates the difference in the growth rate between the crystallographic phases. Therefore, anisotropic growth in the form of nanorods occurs. This idea is confirmed by FTIR measurements on the intermediate. We have observed a similar trend for CdTe nanoparticles.[35]

The HRTEM images of the PbTe nanorods clearly show visible lattice fringes with a lattice spacing of 3.23 Å, assigned to the (200) reflection of cubic PbTe (Figure 8). Selected area electron diffraction patterns (SAED) show the single crystalline nature of both the dots and rods of PbTe. The crystallinity of the PbTe nanoparticles prepared with $PbCO_3$ has been confirmed by powder XRD, which indicates all are halite (fcc, space group *Fm*3*m*) with a lattice constant of a = 6.449 Å. This is consistent with the standard value (a = 6.454 Å) for the bulk face-centred cubic phase of PbTe (ICDD No: 08-0028). The major diffraction peaks are indexed as the (200), (220), (222), (420) and (422) planes of cubic PbTe (Figure 3c). No peaks characteristic of impurities were observed.

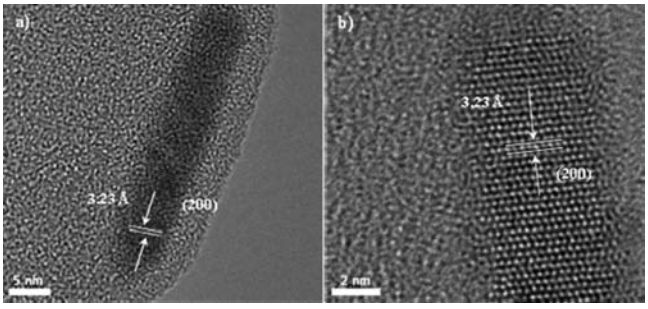

Figure 8. (a) and (b) HRTEM images of PbTe nanorods prepared from lead carbonate at 270 °C after 4 h.

Conclusions

High-quality nanocrystals of PbS, PbSe and PbTe have been prepared by a simple route by using sulfide/selenide/telluride produced from sulfur/selenium/tellurium powder reduced with $NaBH_4$ and lead as the carbonate, nitrate, sulfate and chloride. All the materials prepared have the halite structure as confirmed by powder XRD. The shape of the as-prepared nanoparticles at different temperatures was studied by TEM and HRTEM. The shape of the final product is relatively easy to control and provides a more reliable route to such rods than some earlier approaches.

Experimental Section

All reagents were purchased from Sigma–Aldrich chemical company and used as received. Solvents were distilled prior to use.

Synthesis of PbS Nanoparticles: In a typical procedure, sulfur (0.62 mmol) was mixed with deionized water (20.0 mL) in a three-neck flask. $NaBH_4$ (1.60 mmol) dissolved in deionized water (20.0 mL) was added to this mixture and was left to stir for 12 h under a nitrogen atmosphere at room temperature. The lead salt (0.64 mmol of $PbCO_3$, $(PbNO_3)_2$ or $PbSO_4$) dissolved in deionized water (20.0 mL) was added. The solution was stirred for 30 min, followed by the addition of excess methanol. The resultant solution was then centrifuged and decanted to isolate the solid products, which were dispersed into TOP (6.0 mL) and injected into hot hexadecylamine (HDA) at 230 °C. The reaction was allowed to continue for 2 h. The black solution was cooled to 50 °C. Addition of excess methanol to the solution resulted in the reversible flocculation of the nanoparticles. The flocculate was separated from the supernatant by centrifugation. The resultant particles were dissolved in toluene for characterization.

Synthesis of PbSe and PbTe Nanoparticles: The synthesis of PbSe and PbTe nanoparticles is slightly different from that of PbS; e.g. selenium powder (0.31 mmol) was mixed with deionized water (20.0 mL) in a three-neck flask. $NaBH_4$ (0.80 mmol) was then carefully added, and the flask was immediately purged with nitrogen to facilitate an inert atmosphere. After 1.5 h, lead carbonate (0.31 mmol) was added to the reaction mixture. The suspension was stirred for 30 min, followed by the addition of excess methanol. The resultant suspension was then centrifuged. The precipitate was dispersed in TOP and injected into hot hexadecylamine at 190 °C, and the reaction was allowed to continue for 4 h. The black solution was cooled to 50 °C. Addition of excess methanol resulted in HDA-capped PbSe particles.

The process was repeated by varying the injection temperatures and lead sources (lead chloride and lead nitrate). A similar procedure was followed to prepare the PbTe nanoparticles with tellurium.[31]

Characterization of Nanoparticles: X-ray diffraction studies were performed on a Bruker AXS D8 diffractometer by using Cu-K_α radiation. The samples were mounted flat and scanned between 20 to 80° with a step size of 0.05 and a count rate of 9 s. Transmission electron microscopy analysis was performed by using a JEOL 1010 TEM instrument. High-resolution transmission electron microscopy (HRTEM) was performed with a JEOL 2100 TEM instrument, which operated at 200 kV. Infrared spectra were recorded on a Perkin–Elmer Spectrum BX FTIR spectrometer.

Acknowledgments

K. R. is grateful to ORS and the University of Manchester for financial support. The authors also thank EPSRC, UK for grants to P. O. B. N. R. is grateful to the Department of Science and Technology (DST) and National Research Foundation (NRF) of South Africa through the DST/NRF South African Research Chairs Initiative for Professor of Nanotechnology.

[1] A. P. Alivisatos, *Science* **1996**, *271*, 933.
[2] Y. Wang, N. Herron, *J. Phys. Chem.* **1991**, *95*, 525.
[3] P. Calvert, *Nature* **1999**, *399*, 210.
[4] D. Cui, J. Xu, T. Zhu, G. Paradee, S. Ashok, M. Gerhold, *Appl. Phys. Lett.* **2006**, *88*, 183111.
[5] D. Qi, M. Fischbein, M. Drndic, S. Selmic, *Appl. Phys. Lett.* **2005**, *86*, 093103.
[6] T. C. Harman, P. J. Taylor, M. P. Walsh, B. E. Laforge, *Science* **2002**, *297*, 2229.
[7] F. W. Wise, *Acc. Chem. Res.* **2000**, *33*, 773.
[8] S. A. Mc Donald, G. Konstantatos, S. Zhang, P. W. Cyr, E. J. D. Klem, L. Levina, E. H. Sargent, *Nat. Mater.* **2005**, *4*, 138.
[9] C. B. Murray, S. Sun, W. Gaschler, H. Doyle, T. A. Betley, C. R. Kagan, *IBMJ. Res. Dev.* **2001**, *45*, 47.
[10] W. Lu, J. Fang, Y. Ding, Z. L. Wang, *J. Phys. Chem. B* **2005**, *109*, 19219.
[11] K. Cho, D. V. Talapin, W. Gaschler, C. B. Murray, *J. Am. Chem. Soc.* **2005**, *127*, 7140.
[12] H. Tong, Y. J. Zhu, L. X. Yang, L. Li, L. Zang, *Angew. Chem.* **2006**, *118*, 7903; *Angew. Chem. Int. Ed.* **2006**, *45*, 7739.
[13] W. Z. Wang, Y. Geng, Y. T. Qian, M. R. Ji, X. M. Liu, *Adv. Mater.* **1998**, *10*, 1479.
[14] M. Afzaal, P. O'Brien, *J. Mater. Chem.* **2006**, *16*, 1113.
[15] G. R. Li, C. Z. Yao, X. H. Lu, F. L. Zheng, Z. P. Feng, X. L. Yu, C. Y. Su, Y. X. Tong, *Chem. Mater.* **2008**, *20*, 3306.
[16] R. Kerner, O. Pelchik, A. Gedanken, *Chem. Mater.* **2001**, *13*, 1413.
[17] C. Cheng, G. Hu, H. Zhang, *J. Cryst. Growth* **2009**, *311*, 1285.
[18] S. M. Lee, Y. Jun, S. N. Cho, J. Cheon, *J. Am. Chem. Soc.* **2002**, *124*, 11244.
[19] A. Jdanov, J. Pelleg, Z. Dashevsky, R. Shneck, *Mater. Sci. Eng. B* **2004**, *106*, 89.
[20] J. E. Ge, Y. D. Li, *J. Mater. Chem.* **2003**, *13*, 911.
[21] U. Kumar, S. N. Sharma, S. Singh, M. Kar, V. N. Singh, B. R. Mehta, R. Kakar, *Mater. Chem. Phys.* **2009**, *113*, 107.
[22] T. Trindade, O. C. Monteiro, P. O'Brien, M. Motevalli, *Polyhedron* **1999**, *18*, 1171.
[23] J. Akhtar, M. A. Malik, P. O'Brien, M. Helliwell, *J. Mater. Chem.* **2010**, *20*, 6116.
[24] T. Trindade, P. O'Brien, X.-M. Zhang, M. Motevalli, *J. Mater. Chem.* **1997**, *7*, 1011.
[25] M. J. Moloto, N. Revaprasadu, G. A. Kolawole, P. O'Brien, M. A. Malik, *S. Afr. J. Sci.* **2005**, *101*, 463.
[26] S. N. Moloto, N. Revaprasadu, P. Christian, P. O'Brien, *Mater. Res. Soc. Symp. Proc,* **2005**, *##879E*, Z7.6.
[27] D. Berhanu, K. Govender, D. S. Boyle, M. Archbold, D. P. Halliday, P. O'Brien, *Chem. Commun.* **2006**, 4709.
[28] M. Du, Y. Wang, J. Xu, P. Yang, Y. Du, *Colloid J.* **2008**, *70*, 720.
[29] R. Rhodes, P. O'Brien, B. R. Saunders, *J. Colloid Interface Sci.* **2011**, *358*, 151.
[30] N. Ziqubu, K. Ramasamy, P. V. S. R. Rajasekhar, N. Revaprasadu, P. O'Brien, *Chem. Mater.* **2010**, *22*, 3817.
[31] J. H. Warner, H. Cao, *Nanotechnology* **2008**, *19*, 305605.
[32] S. M. Lee, S. N. Cho, J. Cheon, *Adv. Mater.* **2003**, *15*, 441.
[33] C. J. Murphy, *Science* **2002**, *298*, 2139.
[34] P. J. Thomas, P. O'Brien, *J. Am. Chem. Soc.* **2006**, *128*, 5614.
[35] N. Mntungwa, P. V. S. R. Rajasekhar, N. Revaprasadu, *Mater. Chem. Phys.* **2011**, *126*, 500.

Received: August 5, 2011
Published Online: October 17, 2011

